Electronic Supplementary Material (ESI) for Inorganic Chemistry Frontiers.

Supporting Information

Reversible Tristate Structural Transition within Hybrid Copper (I) Bromides toward Tunable Multiple Emission

Jiajing Wu*, Jing-Li Qi, Yue Guo, Shu-Fang Yan, Wenlong Liu and Sheng-Ping Guo*

[a] School of Chemistry and Chemical Engineering, Yangzhou University, Yangzhou, Jiangsu 225002, P. R. China.

*E-mail: spguo@yzu.edu.cn, jiajingw@yzu.edu.cn.

Contents

Figure S13. Two-dimensional fingerprint plot analysis: The C−H···π interaction of **112** (a), **224** (b) and **246** (c).

Figure S14. Two-dimensional fingerprint plot analysis: The π···π interaction of **112** (a), **224** (b) and **246** (c).

Figure S15. Two-dimensional fingerprint plot analysis: Hydrogen bond of **112** (a), **224** (b) and **246** (c).

Figure S16. Powder XRD patterns of **112** (a), **224** (b), and **246** (c) after immersion in water for three weeks.

Figure S17. Comparison of the solubility of $(EtPh_3P)Br$ in methanol, ethanol, and isopropanol.

Figure S18. Comparison of the solubility of CuBr in methanol, ethanol, and isopropanol.

Figure S19. Photographs of three kinds of **112** samples under 365 nm ultraviolet excitation with the increase of ethanol soaking time. **1** is crystal with heat treatment, **2** is crystal without heat, and **3** is powder without heat.

Figure S20. Structure transformations from **112** to **246**: **112** treated by water (**1**), ethylene glycol (**2**), acetic acid (**3**).

Figure S21. The color of the pH test paper before and after adding **112** (a, c) or **224** (d, f) to the seven solvents(methanol, ethanol, isopropyl alcohol, ethylene glycol, water, acetic acid, formic acid). Luminescence of **112** (b) and **224** (e) in these solvents under 365 nm UV stimulation.

Figure S22. Structure transformations from **224** to **246**: **224** treated by water (**1**), acetic acid (**2**), ethylene glycol (**3**).

Figure S23. The powder XRD patterns of **246** after immersion in methanol, ethanol, and acetic acid for one day, respectively.

Experiment detail

Structural Transformation from 112 (224) to 246: 0.92 mmol (0.46 mmol) **112** (**224**) powder was dispersed in 1.5 mL different solvents including methanol, ethanol, and isopropanol, respectively.

Structural Transformation from 246 (224) to 112: 10 mg (30 mg) **246 (224)** powder and 0.2 g (0.1 g) of $EtPh_3PBr$ were dispersed in 1 mL ethanol and heated at 70 ℃ to form a transparent solution under stirring. As the mixture slowly cooled to room temperature, **112** crystals were precipitated, achieving structural transformation from **246 (224)** to **112**.

Structural Transformation from 246 (112) to 224: 20 mg (30 mg) of **246** (**112**) powders and 0.04 g (0.02 g) of $EtPh_3PBr$ were dispersed in 1 mL ethanol and heated at 70 ℃ under stirring until the solution became clear. As the mixture slowly cooled to room temperature, **224** crystals were precipitated, completing structural transformation from **246** (**112**) to **224**.

Characterizations

The crystallography data of **112**, **224** and **246** were collected using a Bruker D8 QUEST X-ray diffractometer equipped with a graphite-monochromated Mo-Kα radiation (λ = 0.71073 Å). The purity of the samples was confirmed by Powder X-ray diffraction (Bruker D8 Advance) at 40 kV and 100 mA for Cu-Kα radiation (λ = 1.5406 Å) with a scan speed of 5°/min at room temperature within the range of 2θ = 5−60°. An energy dispersive X-ray spectroscope (EDS, Zeiss-Supra55) was used for microprobe elemental analyses. The UV-vis absorption spectroscopy was collected by Cary 5000 at room temperature within the range of 200−600 nm. The photoluminescence excitation (PLE) and photoluminescence (PL) spectra measurements were performed on an F7000 fluorescence spectrophotometer (Hitachi High-Tech Ltd., JP). The PLQY was measured using the integrated sphere on the Edinburgh FLS980 instrument. The PL decay curves were obtained by the FLS920 (Edinburgh, UK).

PL lifetime fitting : Time-resolved PL decay curve of **112** was fitted by formula **1** and the average PL decay lifetime was calculated by formula **2**.

$$I(t) = A_1 e^{\frac{-t}{\tau_1}} + A_2 e^{\frac{-t}{\tau_2}} \quad (1)$$

$$\tau_{ave} = \frac{A_1 {\tau_1}^2 + A_2 {\tau_2}^2}{A_1 \tau_1 + A_2 \tau_2} \quad (2)$$

where A_1 and A_2 are the fitting constants, τ_1 and τ_2 are the exponential components, I is the luminescence intensity and t is the time. Time-resolved PL decay curve of **224** and **246** were fitted by formula **3** and average PL decay lifetime were calculated by formula **4**.

$$I(t) = A e^{\frac{-t}{\tau}} \tag{3}$$

$$\tau_{ave} = \frac{A\tau^2}{A\tau} \tag{4}$$

where A is the fitting constants, τ are the exponential components, I is the luminescence intensity and t is the time.

Calculation of K_r and K_{nr}: The radiative decay rates (K_r) and non-radiative decay rates (K_{nr}) of the three compounds were calculated by formulae **5** and **6**.

$$\Phi = \frac{k_r}{k_r + k_{nr}} \tag{5}$$

$$\tau = \frac{1}{k_r + k_{nr}} \tag{6}$$

Where Φ stands for PLQY, K_r stands for radiative carrier recombination rate, K_{nr} stands for nonradiative carrier recombination rate, τ stands for an average lifetime.

The detailed results of fitting parameter, K_r, and K_{nr} are listed in Table S8.

Table S1. Crystal data and structure refinement for **112**, **224**, and **246**.

Compound	112	224	246
Formula weight	514.69	1029.38	1304.56
Temperature/K	296	296	296
Crystal system	monoclinic	monoclinic	monoclinic
Space group	$P2_1$	$P2_1/c$	$P2_1/n$
a/Å	9.7557(4)	8.8726(4)	10.5061(7)
b/Å	12.2416(5)	20.0303(9)	13.6196(8)
c/Å	9.7625(4)	11.3005(5)	15.6666(11)
α/°	90	90	90
β/°	118.6090(10)	94.7890(10)	96.123(2)
γ/°	90	90	90
Volume/Å^3	1023.54(7)	2001.32(16)	2228.9(3)
Z	2	2	2
ρ_{calc}/g·cm^{-3}	1.67	1.708	1.944
μ/mm^{-1}	5.048	5.163	7.245
F(000)	508	1016	1262
Radiation	MoKα (λ = 0.71073)	MoKα (λ = 0.71073)	MoKα (λ = 0.71073)
2θ range for data collection/°	4.752 to 59.372	4.15 to 56.732	4.458 to 59.26
Reflections collected	16823	32201	36413
Data/restraints/ parameters	5718/1/218	5002/0/218	6263/0/282
Goodness-of-fit on F^2	1.019	0.999	1.008
Final R indexes [I>=2σ (I)]	R1 = 0.0419, wR2 = 0.0758	R1 = 0.0453, wR2 = 0.0664	R1 = 0.0441, wR2 = 0.0649
Final R indexes [all data]	R1 = 0.0846, wR2 = 0.0865	R1 = 0.1098, wR2 = 0.0795	R1 = 0.1077, wR2 = 0.0780

R1 = $\Sigma||F_o|-|F_c|| / \Sigma|Fo|$, wR2 = $\{\Sigma[w(|F_o|^2 - |F_c|^2)^2] / \Sigma[w(|F_o|^4)]^{1/2}$ and $w = 1/[\sigma^2(F_o^2)+(0.0462P)^2]$ where $P = (F_o^2+2F_c^2)/3$

Table S2. Fractional atomic coordinates (× 10^4) and equivalent isotropic displacement parameters (Å^2 × 10^3) for **224**.

Atom	*x*	*y*	*z*	U_{eq}
Cu (1)	187.4(6)	5569.4(2)	9261.2(4)	66.04(16)
Br (1)	527.9(4)	6475.0(2)	8029.7(3)	54.32(12)
Br (2)	2115.1(5)	4750.9(2)	9867.1(4)	64.07(14)
P(1)	3174.4(9)	3220.9(4)	5945.8(7)	35.5(2)
C (1)	1531(5)	2316.9(18)	4447(3)	64.0(11)
C (2)	2644(4)	2378.9(16)	5528(3)	45.8(8)
C (3)	4097(4)	3631.0(15)	4792(3)	38.1(8)
C (4)	3275(4)	3807.9(17)	3740(3)	48.4(9)
C (5)	4009(5)	4097.7(18)	2839(3)	60.8(11)
C (6)	5540(5)	4209.5(19)	2979(4)	66.7(12)
C (7)	6351(5)	4041.2(19)	4018(4)	63.6(11)
C (8)	5632(4)	3754.0(17)	4925(3)	48.0(9)
C (9)	4466(3)	3188.8(16)	7258(3)	38.4(8)
C (10)	4475(4)	3698.7(19)	8073(3)	55.5(10)
C (11)	5521(5)	3693(2)	9059(3)	68.5(12)
C (12)	6534(4)	3183(3)	9224(3)	67.3(12)
C (13)	6520(4)	2674(2)	8422(4)	62.2(11)
C (14)	5501(4)	2668.2(17)	7439(3)	50.8(9)
C (15)	1538(3)	3692.7(15)	6247(3)	35.5(7)
C (16)	1542(4)	4380.8(17)	6129(3)	48.6(9)
C (17)	351(4)	4754.2(18)	6473(3)	55.5(10)
C (18)	-834(4)	4449(2)	6923(3)	58.6(10)
C (19)	-866(4)	3766(2)	7030(3)	61.3(10)
C (20)	316(4)	3382.4(17)	6698(3)	44.6(8)

U_{eq} is defined as 1/3 of the trace of the orthogonalised U_{ij} tensor.

Table S3. Bond angles for **224**.

Atom	Atom	Atom	Angle/°	Atom	Atom	Atom	Angle/°
Cu (1)	Br (2)	Cu (1^{1})	72.29(2)	Cu (1^{1})	Br (2^{1})	Cu (1)	72.29(2)
Br (1)	Cu (1)	Br (2^{1})	127.30(3)	Br (1^{1})	Cu (1^{1})	Br (2)	127.30(3)
Br (1)	Cu (1)	Br (2)	124.98(3)	Br (1^{1})	Cu (1^{1})	Br (2^{1})	124.98(3)
Br (1)	Cu (1)	Cu (1^{1})	178.45(3)	Br (1^{1})	Cu (1^{1})	Cu (1)	178.45(3)
Br (2)	Cu (1)	Br (2^{1})	107.71(2)	Br (2^{1})	Cu (1^{1})	Br (2)	107.71(2)
Br (2)	Cu (1)	Cu (1^{1})	53.874(19)	Br (2^{1})	Cu (1^{1})	Cu (1)	53.874(19)
Br ($2^{1)}$	Cu (1)	Cu (1^{1})	53.838(19)	Br (2)	Cu (1^{1})	Cu (1)	53.838(19)

Table S4. Bond lengths for **224**.

Atom	Atom	Length/Å	Atom	Atom	Length/Å
Cu (1)	Br (1)	2.3213(6)	Cu (1^{1})	Br (1^{1})	2.3213(6)
Cu (1)	Br (2)	2.4262(6)	Cu (1^{1})	Br (2^{1})	2.4262(6)
Cu (1)	Br (2^{1})	2.4273(7)	Cu (1^{1})	Br (2)	2.4273(7)
Cu (1)	Cu (1^{1})	2.8627(10)	Cu (1^{1})	Cu (1)	2.8627(10)

Table S5. Bond angles for **246**.

Atom	Atom	Atom	Angle/°	Atom	Atom	Atom	Angle/°
Cu (2)	Br (4)	Cu (3)	71.65(19)	Br (1)	Cu (4)	Cu (2)	106.07(17)
Cu (2)	Br (5)	Cu (4)	69.90(19)	Br (4)	Cu (3)	Br (6)	123.9(3)
Cu (4)	Br (6)	Cu (3)	70.90(18)	Br (4)	Cu (3)	Cu (1)	104.4(2)
Cu (3)	Cu (1)	Cu (4)	60.02(3)	Br (4)	Cu (3)	Cu (4)	105.7(2)
Cu (2)	Cu (1)	Cu (4)	59.95(3)	Br (4)	Cu (3)	Cu (2)	53.5(2)
Cu (2)	Cu (1)	Cu (3)	60.72(3)	Br (4)	Cu (3)	Br (2)	117.3(3)
Br (1)	Cu (1)	Cu (4)	56.76(16)	Br (6)	Cu (3)	Cu (1)	103.9(2)
Br (1)	Cu (1)	Cu (3)	109.0(2)	Br (6)	Cu (3)	Cu (4)	52.95(17)
Br (1)	Cu (1)	Cu (2)	107.55(13)	Br (6)	Cu (3)	Cu (2)	106.50(14)
Br (2)	Cu (1)	Cu (4)	108.69(19)	Br (6)	Cu (3)	Br (2)	118.7(3)
Br (2)	Cu (1)	Cu (3)	56.06(17)	Cu (1)	Cu (3)	Cu (4)	60.15(3)
Br (2)	Cu (1)	Cu (2)	107.9(2)	Cu (1)	Cu (3)	Cu (2)	59.32(3)
Br (2)	Cu (1)	Br (1)	122.4(3)	Cu (4)	Cu (3)	Cu (2)	59.54(3)
Br (3)	Cu (1)	Cu (4)	110.23(17)	Br (2)	Cu (3)	Cu (1)	54.57(15)
Br (3)	Cu (1)	Cu (3)	111.7(2)	Br (2)	Cu (3)	Cu (4)	107.51(18)
Br (3)	Cu (1)	Cu (2)	59.3(2)	Br (2)	Cu (3)	Cu (2)	105.43(19)
Br (3)	Cu (1)	Br (1)	117.3(3)	Br (4)	Cu (2)	Br (5)	122.2(2)
Br (3)	Cu (1)	Br (2)	119.6(3)	Br (4)	Cu (2)	Cu (1)	106.16(15)
Br (5)	Cu (4)	Cu (1)	104.8(2)	Br (4)	Cu (2)	Cu (4)	107.28(19)
Br (5)	Cu (4)	Cu (3)	107.0(2)	Br (4)	Cu (2)	Cu (3)	54.90(18)
Br (5)	Cu (4)	Cu (2)	53.6(2)	Br (4)	Cu (2)	Br (3)	119.5(2)
Br (5)	Cu (4)	Br (1)	117.0(3)	Br (5)	Cu (2)	Cu (1)	108.0(2)
Br (6)	Cu (4)	Br (5)	125.1(3)	Br (5)	Cu (2)	Cu (4)	56.5(2)
Br (6)	Cu (4)	Cu (1)	106.24(16)	Br (5)	Cu (2)	Cu (3)	109.0(2)
Br (6)	Cu (4)	Cu (3)	56.15(14)	Br (5)	Cu (2)	Br (3)	118.3(2)
Br (6)	Cu (4)	Cu (2)	110.21(17)	Cu (1)	Cu (2)	Cu (4)	60.50(3)
Br (6)	Cu (4)	Br (1)	117.9(3)	Cu (1)	Cu (2)	Cu (3)	59.95(3)
Cu (3)	Cu (4)	Cu (1)	59.83(3)	Cu (4)	Cu (2)	Cu (3)	59.94(3)
Cu (2)	Cu (4)	Cu (1)	59.54(3)	Br (3)	Cu (2)	Cu (1)	53.37(15)
Cu (2)	Cu (4)	Cu (3)	60.52(3)	Br (3)	Cu (2)	Cu (4)	105.72(16)
Br (1)	Cu (4)	Cu (1)	55.42(13)	Br (3)	Cu (2)	Cu (3)	106.00(13)
Br (1)	Cu (4)	Cu (3)	107.70(16)				

Table S6. Fractional atomic coordinates (× 10^4) and equivalent isotropic displacement parameters (Å^2 × 10^3) for **246**.

Atom	*x*	*y*	*z*	U(eq)
Br (4)	2765(9)	5951(6)	5564(4)	50.7(11)
Br (5)	6233(6)	5124(7)	6770(4)	54.1(8)
Br (6)	4047(8)	3052(4)	5274(5)	61.2(12)
P(1)	2359.2(7)	9181.7(6)	6529.6(5)	37.3(2)
Cu (1)	5664.8(8)	5345.1(6)	4155.5(5)	50.5(2)
Cu (4)	5787.8(8)	4086.2(6)	5522.9(5)	50.3(2)
Cu (3)	3467.1(8)	4654.3(6)	4721.4(6)	52.0(2)
Cu (2)	4991.5(9)	5971.6(6)	5686.6(6)	56.6(2)
C (1)	3759(3)	8848(2)	7219.4(19)	37.7(7)
C (13)	2766(3)	9404(2)	5463.8(18)	35.3(7)
C (6)	4580(3)	8149(2)	6953(2)	49.4(8)
C (7)	1204(3)	8221(2)	6529(2)	43.5(8)
C (14)	2867(3)	8639(2)	4895(2)	47.6(8)
C (16)	3438(3)	9766(3)	3837(2)	51.7(9)
C (18)	3038(3)	10347(2)	5212(2)	51.5(9)
C (2)	4053(4)	9283(3)	8005(2)	68.0(11)
C (19)	1665(3)	10274(2)	6931(2)	53.9(9)
C (15)	3208(3)	8823(2)	4084(2)	54.7(9)
C (8)	1134(4)	7700(3)	7276(2)	61.1(10)
C (17)	3371(4)	10521(2)	4402(2)	60.6(10)
C (12)	341(4)	8027(3)	5826(3)	74.1(12)
C (5)	5665(3)	7896(3)	7474(3)	62.9(10)
C (4)	5950(4)	8337(3)	8254(3)	67.2(11)
C (20)	475(4)	10612(3)	6367(2)	83.3(14)
C (3)	5147(4)	9021(3)	8517(3)	81.5(13)
C (9)	197(4)	7008(3)	7314(3)	85.1(14)
C (11)	-603(4)	7328(4)	5870(3)	95.2(15)
C (10)	-672(4)	6831(3)	6624(4)	90.6(15)
Br (1)	7346(9)	4125(6)	4447(3)	49.3(10)
Br (2)	3757(6)	5021(7)	3245(4)	65.0(15)
Br (3)	6122(8)	6960(4)	4632(4)	57.3(10)

Ueq is defined as 1/3 of the trace of the orthogonalised U_{ij} tensor.

Table S7. Bond lengths for **246**.

Atom	Atom	Length/Å	Atom	Atom	Length/Å
Br (4)	Cu (3)	2.369(6)	Cu (2)	Br (3)	2.524(9)
Br (4)	Cu (2)	2.326(9)	Cu (1)	Br (1)	2.433(6)
Br (5)	Cu (4)	2.416(8)	Cu (1)	Br (2)	2.375(6)
Br (5)	Cu (2)	2.333(8)	Cu (1)	Br (3)	2.356(6)
Br (6)	Cu (4)	2.308(7)	Cu (4)	Cu (3)	2.7326(12)
Br (6)	Cu (3)	2.402(6)	Cu (4)	Cu (2)	2.7213(12)
Cu (1)	Cu (4)	2.7362(11)	Cu (4)	Br (1)	2.471(7)
Cu (1)	Cu (3)	2.7275(12)	Cu (3)	Cu (2)	2.7484(12)
Cu (1)	Cu (2)	2.7100(12)	Cu (3)	Br (2)	2.418(7)

Table S8. The fitting parameters and calculated average PL lifetime, PLQY**,** Radiative (K_r), and nonradiative (K_{nr}) decay rates of of **112**, **224**, and **246**.

Sample	A_1	τ_1 (μs)	A_2	τ_2 (μs)	τ_{avg} (μs)	PLQY (%)	K_r (μs^{-1})	K_{nr} (μs^{-1})	K_r/K_{nr}
112	0.76	2.21	0.26	231.18	225.72	8.7	0.0004	0.0040	0.0953
224	1.08	13.67	-	-	13.67	22.4	0.0164	0.0568	0.2887
246	1.08	37.90	-	-	37.90	76.6	0.0202	0.0062	3.2735

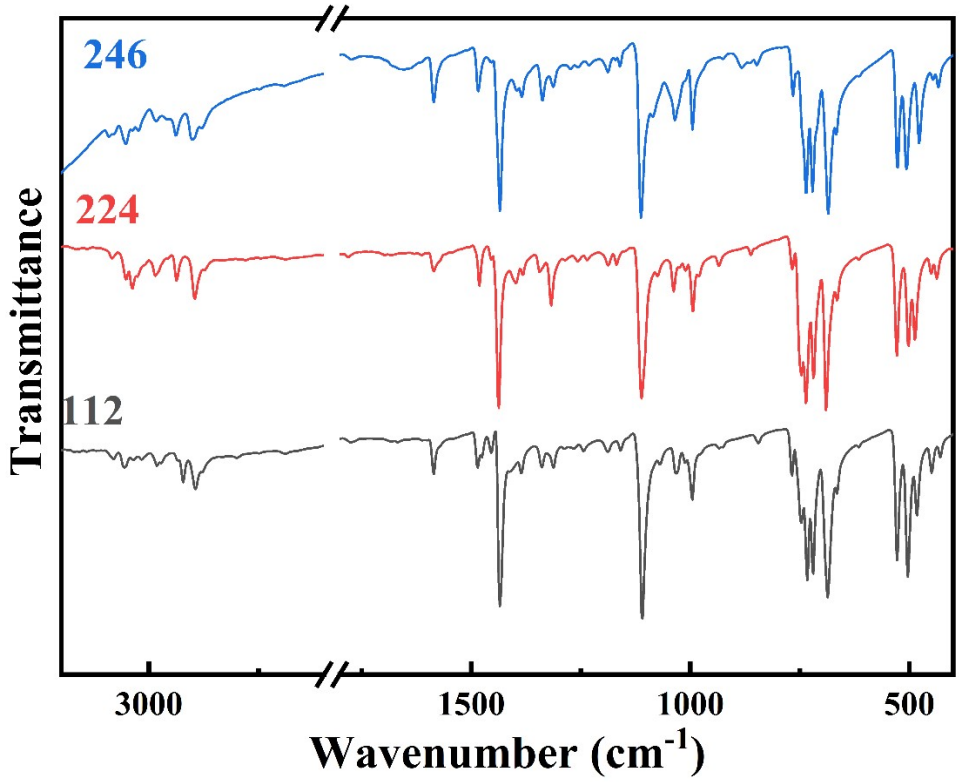

Figure S1. FTIR spectra of **112**, **224** and **246**.

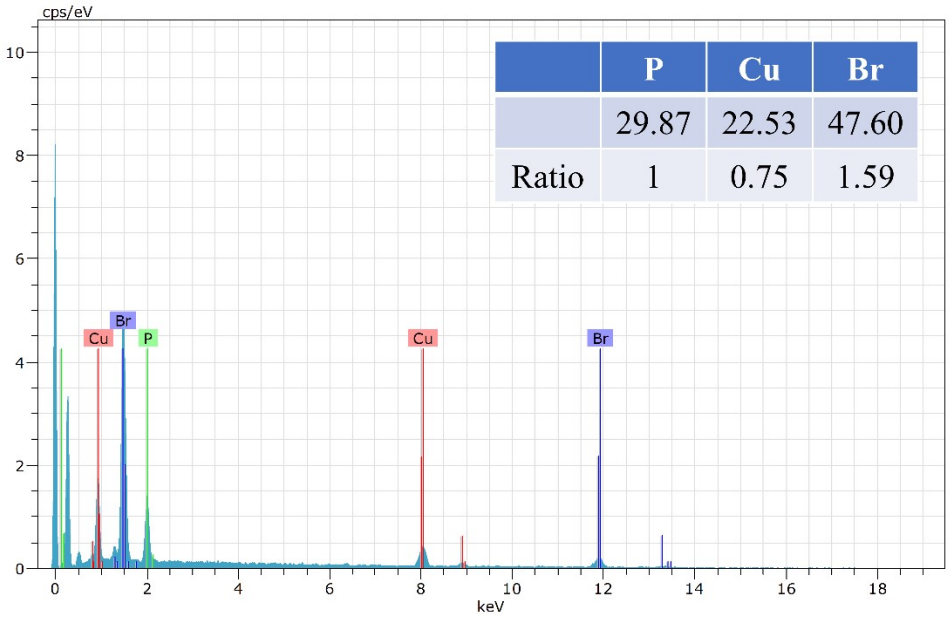

	P	Cu	Br
	29.87	22.53	47.60
Ratio	1	0.75	1.59

Figure S2. The EDS analysis for **112**.

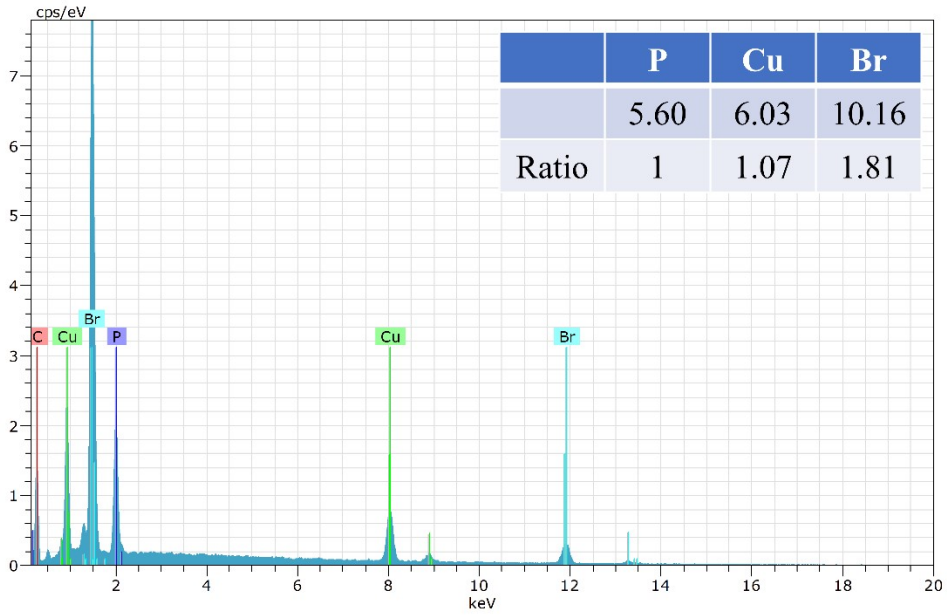

Figure S3. The EDS analysis for **224**.

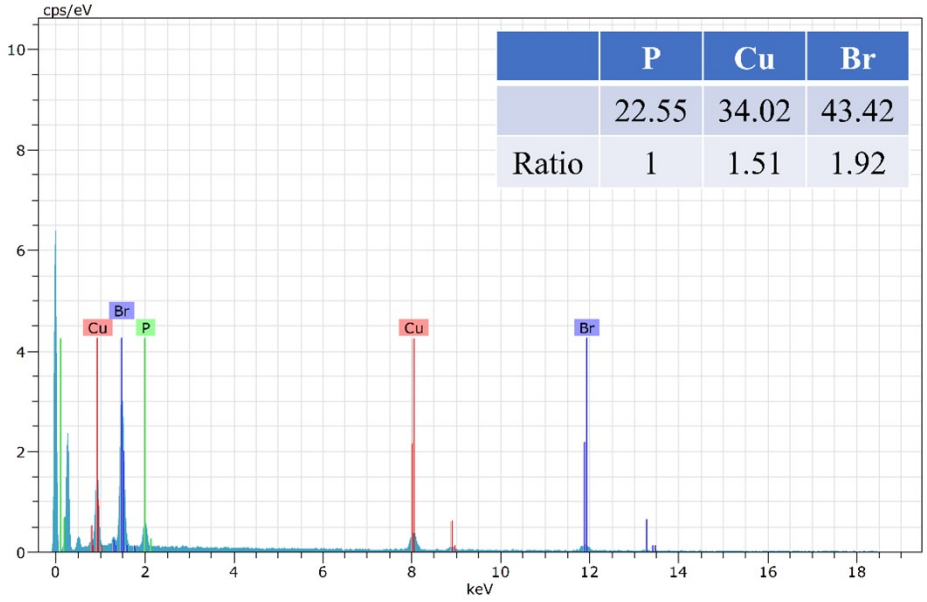

Figure S4. The EDS analysis for **246**.

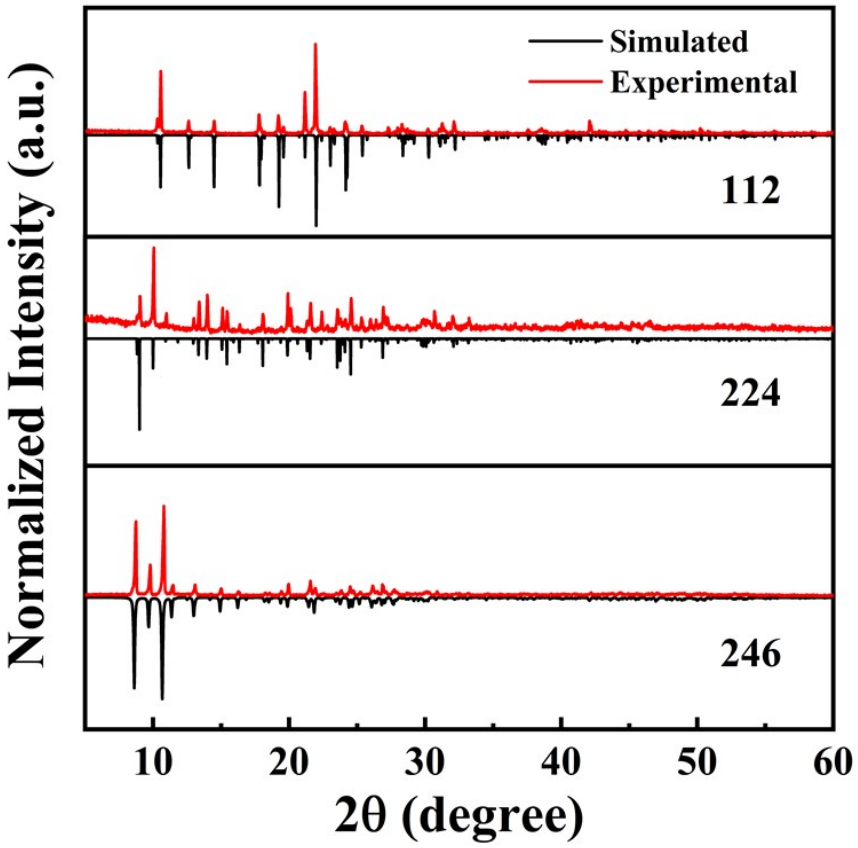

Figure S5. The XRD patterns of **112**, **224** and **246**.

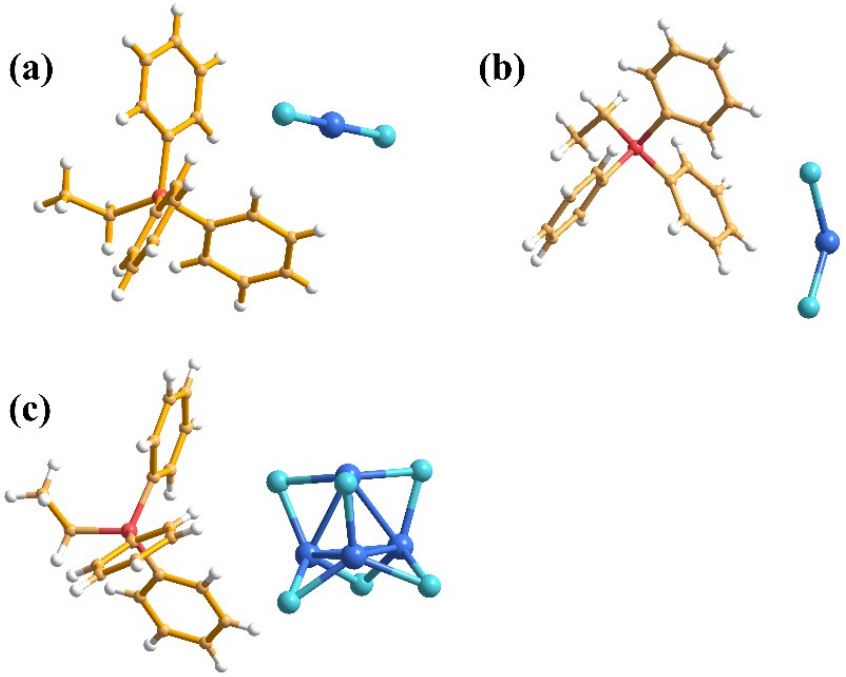

Figure S6. The asymmetric units of **112**, **224** and **246**.

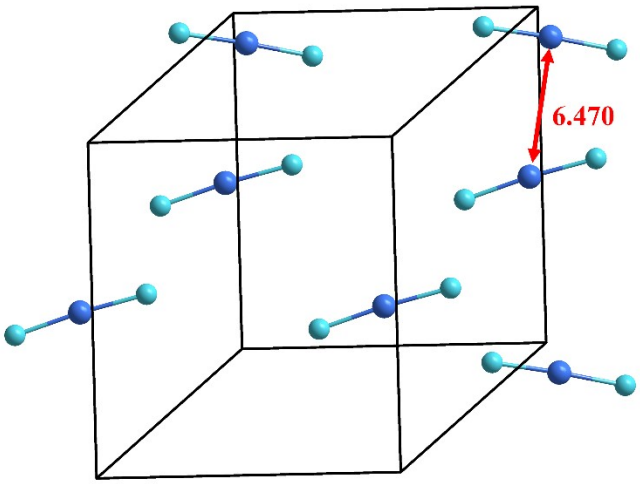

Figure S7. The shortest distance between two adjacent inorganic units in **112**.

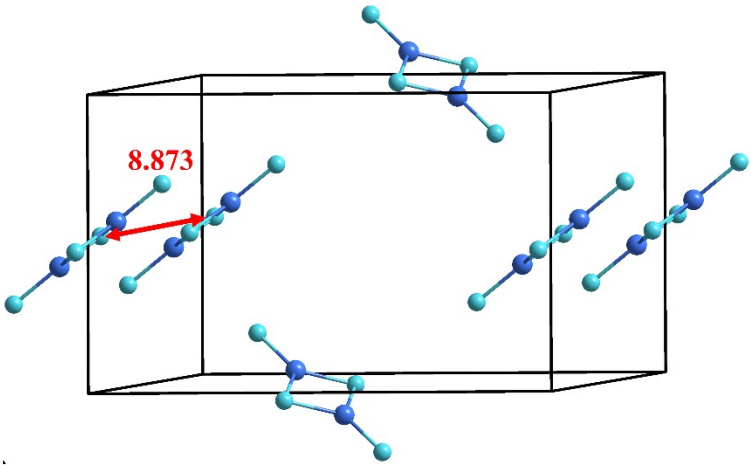

Figure S8. The shortest distance between two adjacent inorganic units in **224**.

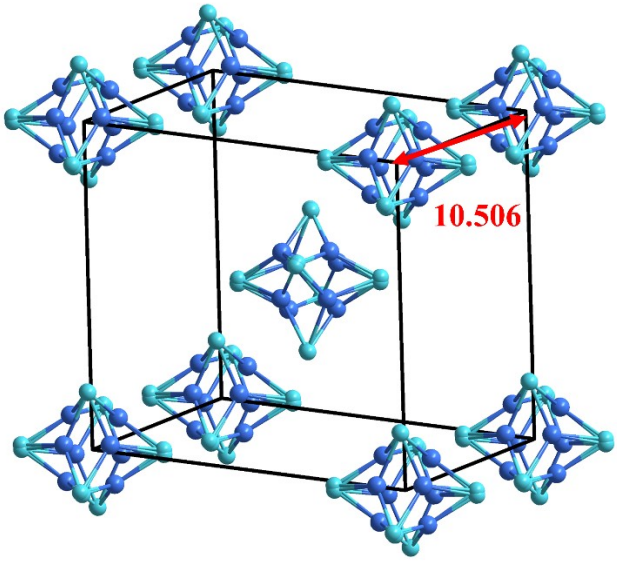

Figure S9. The shortest distance between two adjacent inorganic units in **246**.

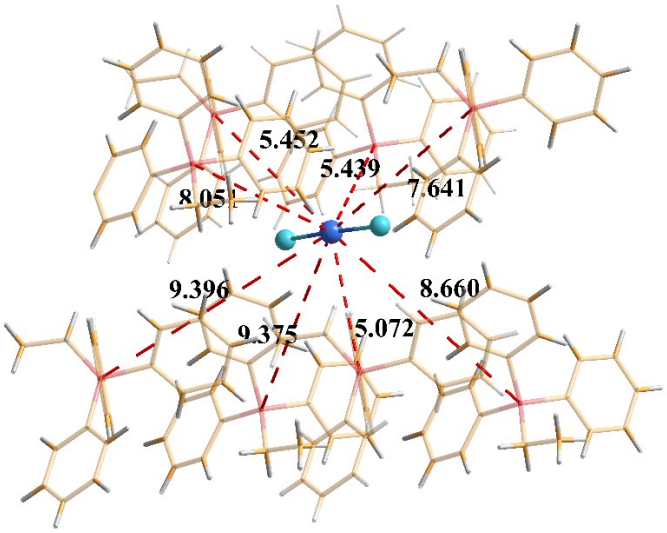

Figure S10. Distance (< 10 Å) between the inorganic units and the surrounding organic cations in **112**.

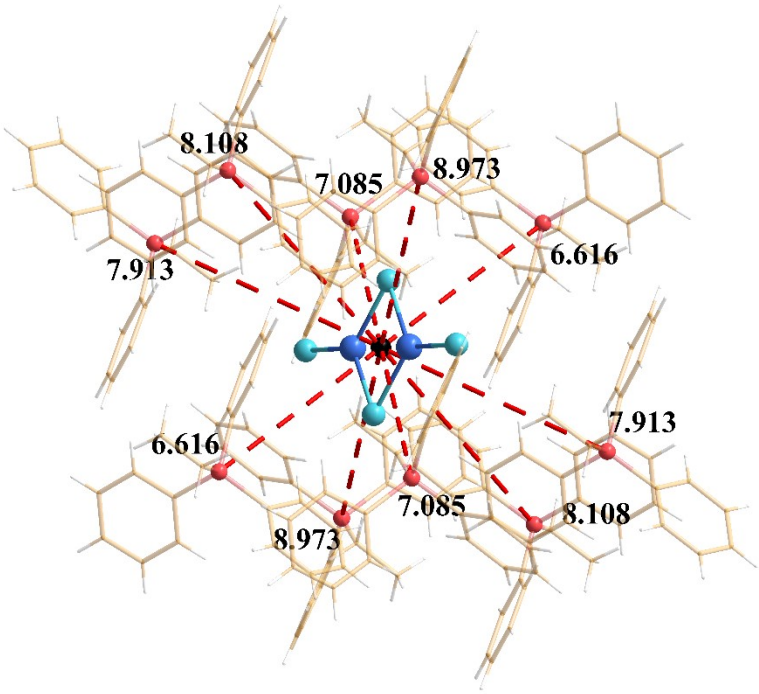

Figure S11. Distance (< 10 Å) between the inorganic units and the surrounding organic cations in **224**.

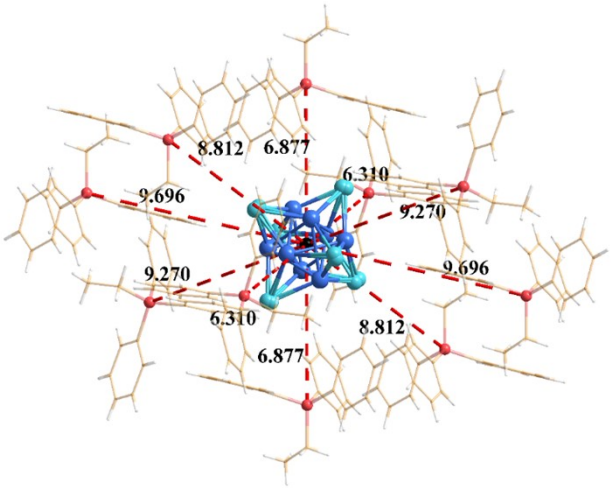

Figure S12. Distance (< 10 Å) between the inorganic units and the surrounding organic cations in **246**.

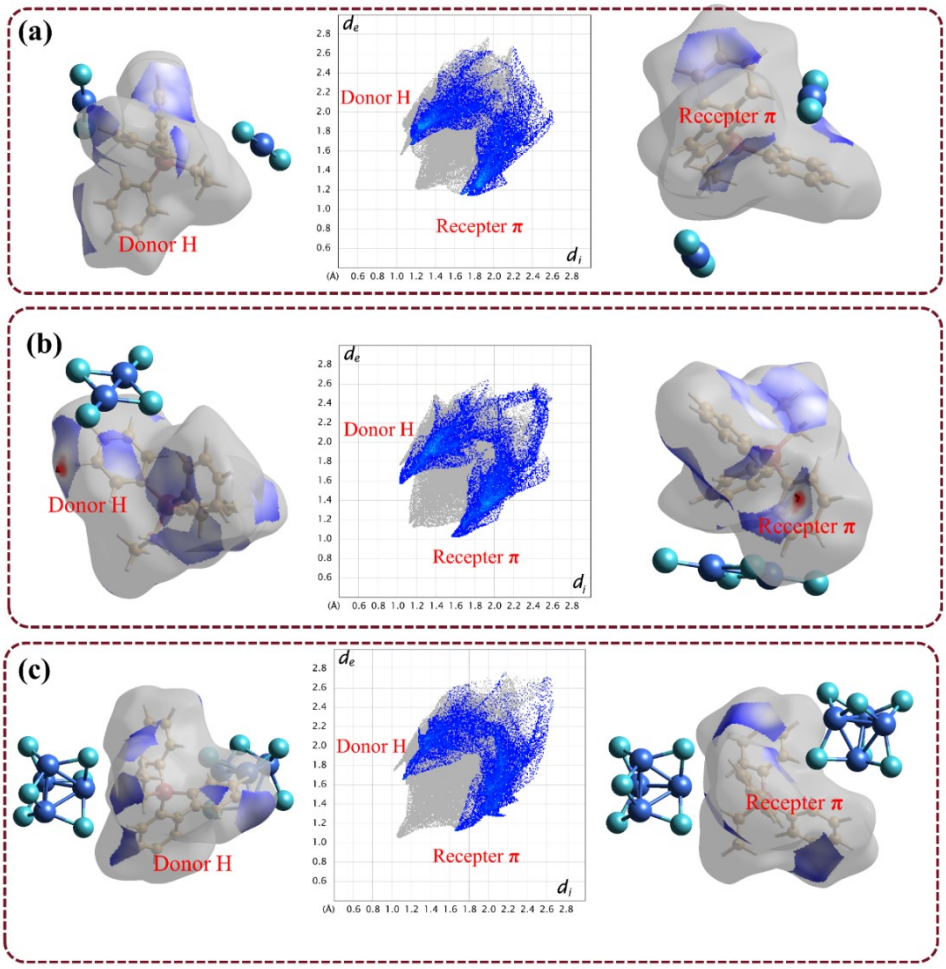

Figure S13. Two-dimensional fingerprint plot analysis: The C–H···π interaction of **112** (a), **224** (b) and **246** (c).

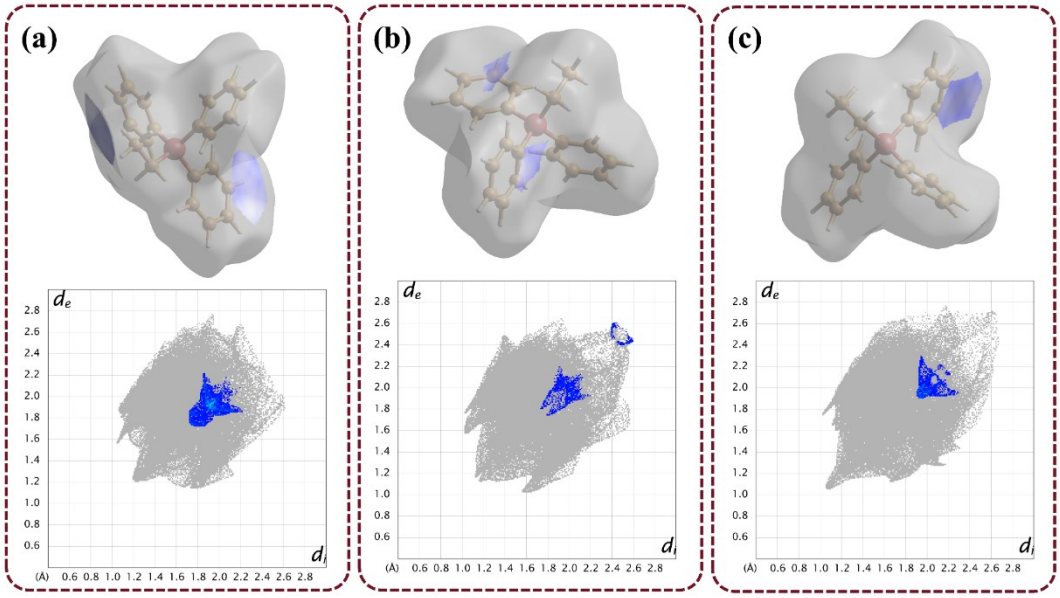

Figure S14. Two-dimensional fingerprint plot analysis: The π···π interaction of **112** (a), **224** (b) and **246** (c).

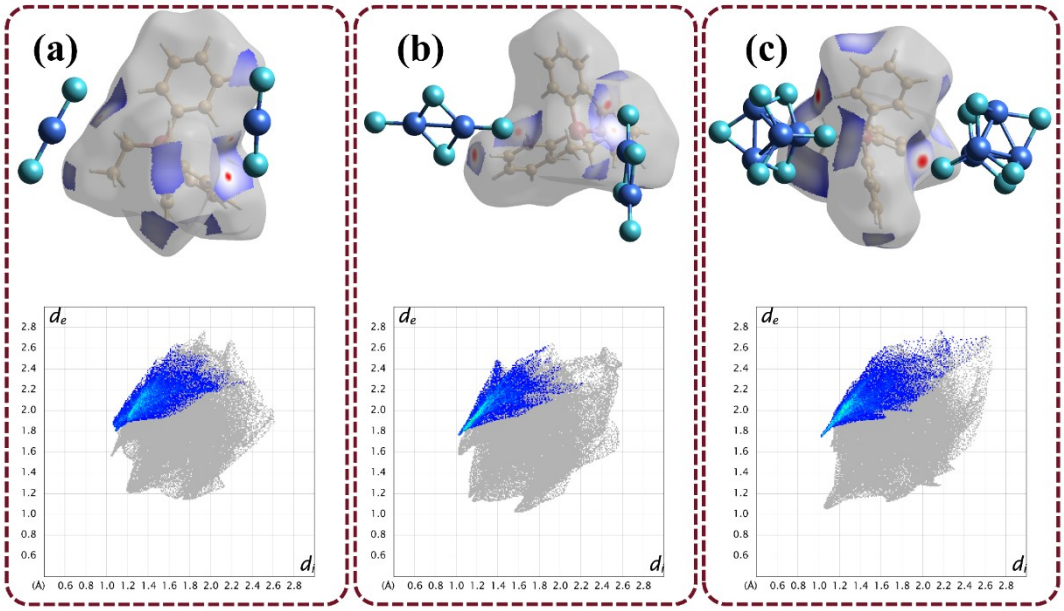

Figure S15. Two-dimensional fingerprint plot analysis: Hydrogen bond of **112** (a), **224** (b) and **246** (c).

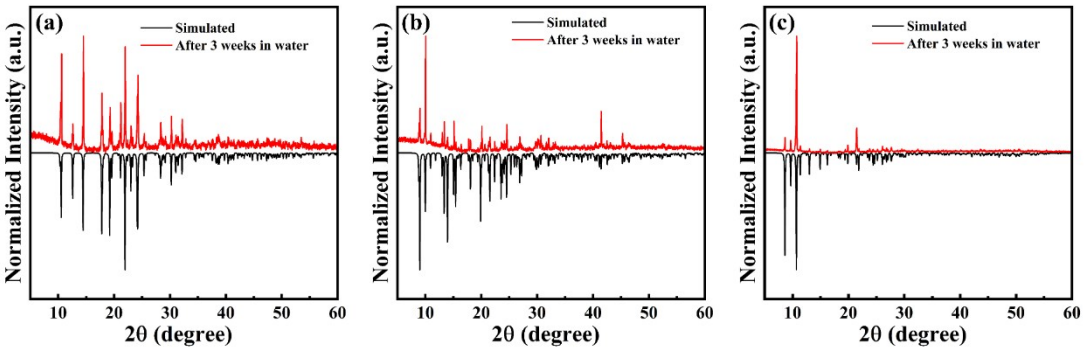

Figure S16. Powder XRD patterns of **112** (a), **224** (b), and **246** (c) after immersion in water for three weeks.

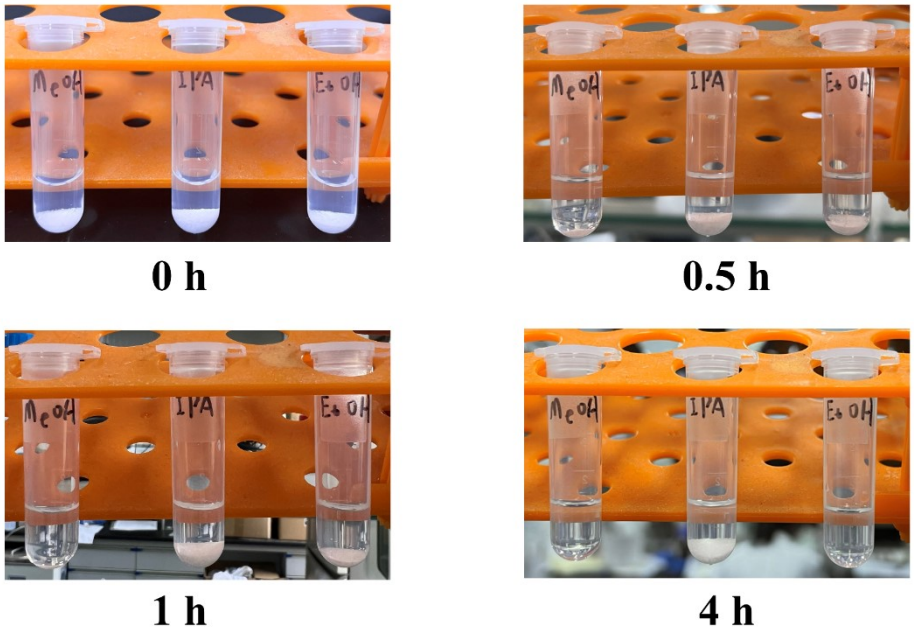

Figure S17. Comparison of the solubility of $(EtPh_3P)Br$ in methanol, ethanol, and isopropanol.

Figure S18. Comparison of the solubility of CuBr in methanol, ethanol, and isopropanol.

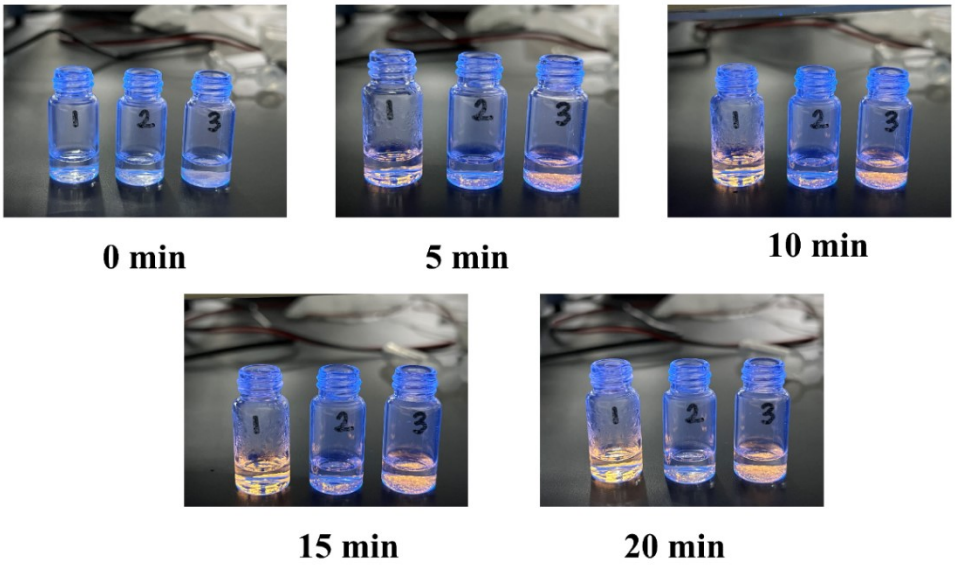

Figure S19. Photographs of three kinds of $(EtPh_3P)CuBr_2$ samples under 365 nm ultraviolet excitation with the increase of ethanol soaking time. **1** is crystal with heat treatment, **2** is crystal without heat, and **3** is powder without heat.

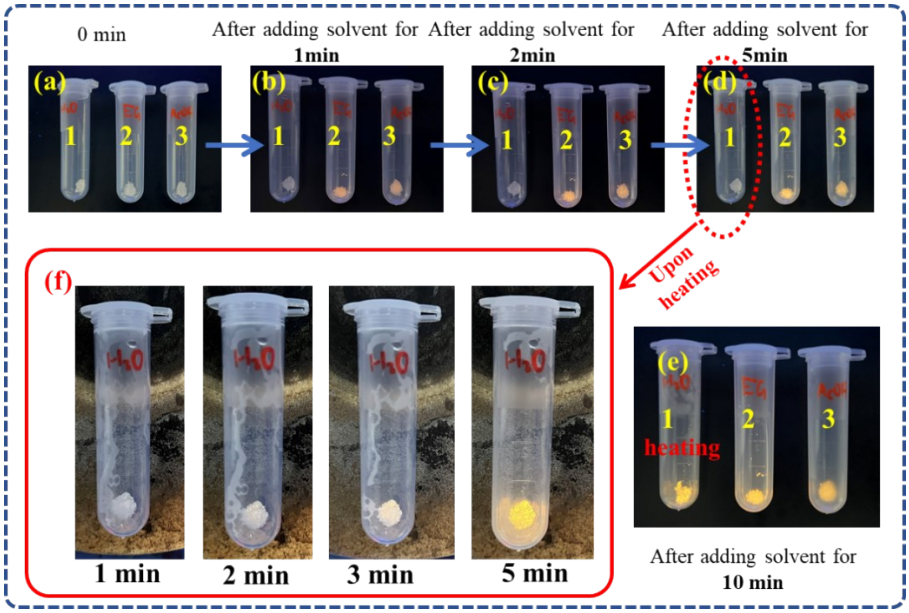

Figure S20. Structure transformations from **112** to **246**: (a−d) Time-dependent optical photographs of **112** treated by water (**1**), ethylene glycol (**2**), acetic acid (**3**); (e) Optical photographs of **112** treated water treated with water (10 minutes under room temperature and 5 minutes under 85 °C), ethylene glycol (15 minutes under room temperature) and acetic acid (15 minutes under room temperature); (f)Time-dependent optical photographs of **112** treated by water with heating.

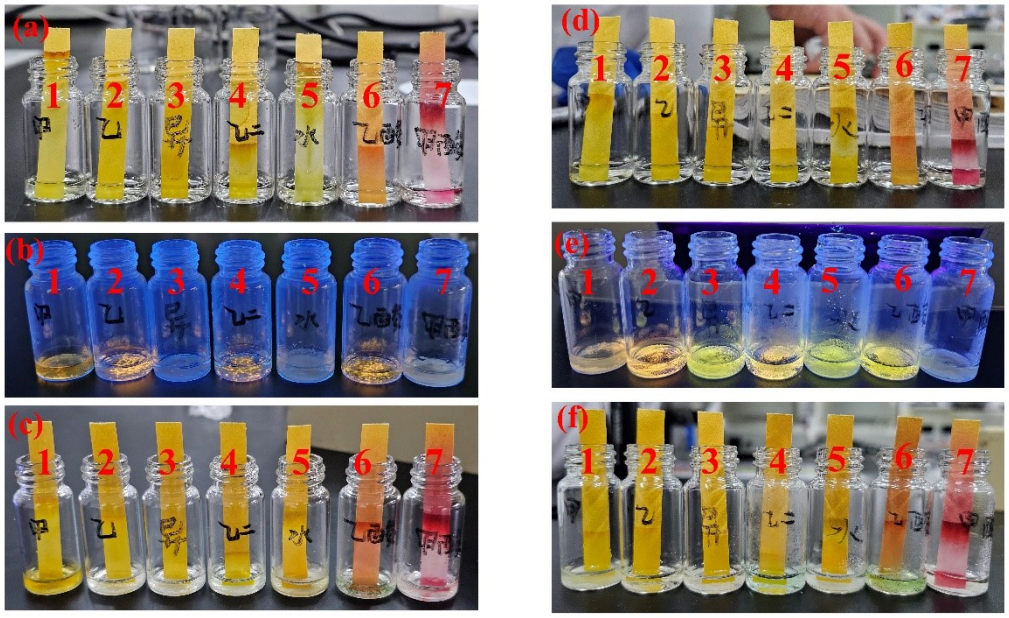

Figure S21. The color of the pH test paper before and after adding **112** (a, c) or **224** (d, f) to the seven solvents (1 is methanol, 2 is ethanol, 3 is isopropyl alcohol, 4 is ethylene glycol, 5 is water, 6 is acetic acid, 7 is formic acid). Luminescence of **112** (b) and **224** (e) in these solvents under 365 nm UV stimulation.

Note:

The pH paper in formic acid and acetic acid turn red, and the approximate pH are 2 and 3 (Fig. S21a and c). Only **112** in acetic acid exhibits yellow emission under 365 nm UV stimulation, indicating that acetic acid can promote the conversion of **112** to **246**, but formic acid cannot (Fig. S21b). The color of the pH paper for the four alcohols (methanol, ethanol, isopropyl alcohol, ethylene glycol), and water, are yellow, indicating that they are neutral (Fig. S21a and c). Under 365 nm UV stimulation, **112** turns to **246** and emits yellow emission in the four alcohols but not in water. This is because the solubility of $(EtPh_3P)Br$ in alcohol is greater than the solubility in water. But in heated water, **112** can also be converted into **246** which is attributed to the increased solubility of $(EtPh_3P)Br$. Based on the above results, neutral or appropriate acidity solvents can induce the conversion of **112** into **246**, such as methanol, acetic acid, etc. But not in more acidic solvents, such as formic acid. The same phenomenon can be observed in **224** (Fig. S21 d-f).

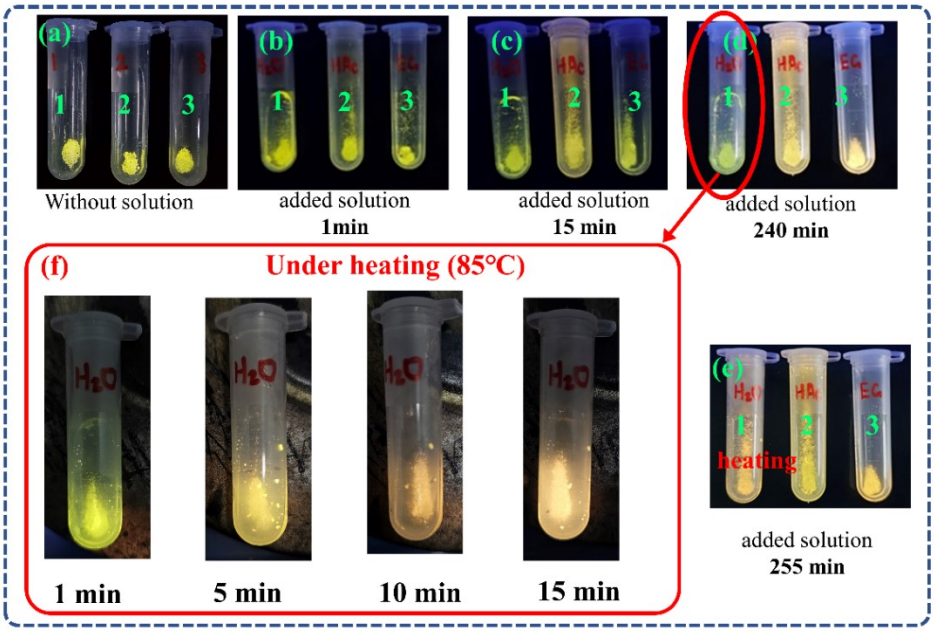

Figure S22. Structure transformation from **224** to **246**. (a-d) Time-dependent optical photographs of **224** treated by water (**1**), acetic acid (**2**), and ethylene glycol (**3**); (e) Optical photographs of **224** treated with water (240 minutes under room temperature and 15 minutes under 85 ℃), ethylene glycol (255 minutes under room temperature) and acetic acid (255 minutes under room temperature); (f) Time-dependent optical photographs of **224** treated by water with heating.

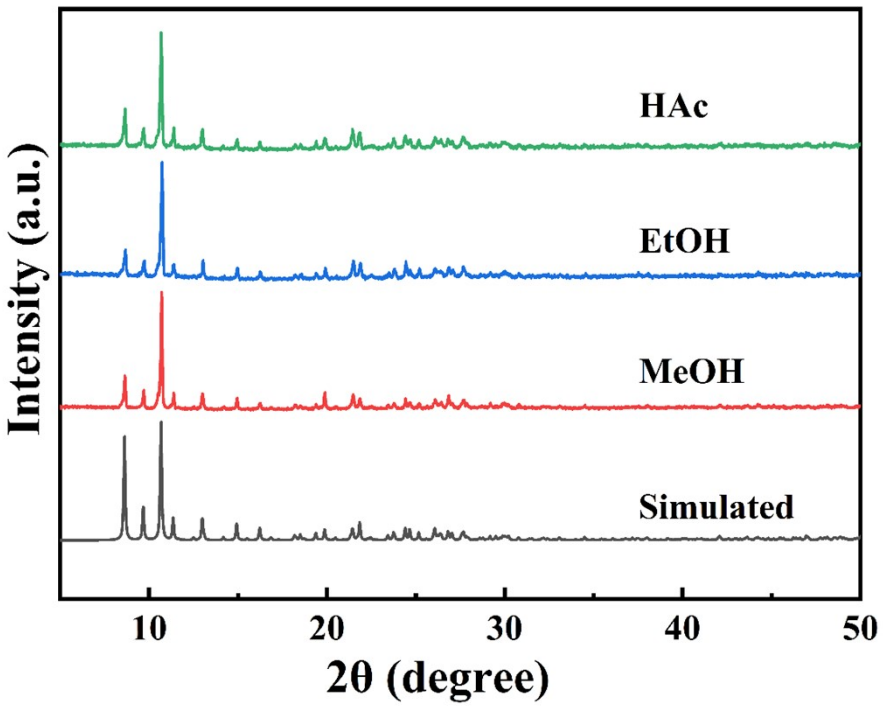

Figure S23. The powder XRD patterns of **246** after immersion in methanol, ethanol, and acetic acid for one day, respectively.